Hindawi
International Journal of Differential Equations
Volume 2022, Article ID 9123178, 9 pages
https://doi.org/10.1155/2022/9123178

Research Article

Bernstein Collocation Method for Solving MHD Jeffery–Hamel Blood Flow Problem with Error Estimations

Ahmad Sami Bataineh,[1] **Osman Rasit Isik**,[2] **and Ishak Hashim**[3]

[1]*Department of Mathematics, Faculty of Science, Al-Balqa Applied University, As-Salt 19117, Jordan*
[2]*Elementary Mathematics Education Program, Faculty of Education, Mugla Sitki Kocman University, 48000 Mugla, Turkey*
[3]*Department of Mathematical Sciences, Faculty of Science & Technology, Universiti Kebangsaan Malaysia, 43650 UKM Bangi, Selangor, Malaysia*

Correspondence should be addressed to Ahmad Sami Bataineh; a_s_bataineh@bau.edu.jo

Received 6 March 2022; Revised 23 March 2022; Accepted 1 April 2022; Published 11 May 2022

Academic Editor: Giovanni P. Galdi

In this paper, the Bernstein collocation method (BCM) is used for the first time to solve the nonlinear magnetohydrodynamics (MHD) Jeffery–Hamel arterial blood flow issue. The flow model described by nonlinear partial differential equations is first transformed to a third-order one-dimensional equation. By using the Bernstein collocation method, the problem is transformed into a nonlinear system of algebraic equations. The residual correction procedure is used to estimate the error; it is simple to use and can be used even when the exact solution is unknown. In addition, the corrected Bernstein solution can be found. As a consequence, the solution is estimated using a numerical approach based on Bernstein polynomials, and the findings are verified by the 4th-order Runge–Kutta results. Comparison with the homotopy perturbation method shows that the present method gives much higher accuracy. The accuracy and efficiency of the proposed method were supported by the analysis of variance (ANOVA) and 95% of confidence on interval error. Finally, the results revealed that the MHD Jeffery–Hamel flow is directly proportional to the product of the angle between the plates α and Reynolds number Re.

1. Introduction

Jeffery and Hamel were the first to study viscous incompressible flow through a channel, which is today known as Jeffery–Hamel flow [1]. Hamel looked at an accurate nonsteady solution of the Navier–Stokes equations (NSE), which describes the process of a vortex decaying due to viscous action [2]. In the special situation of two-dimensional flow through a channel with oblique plane walls meeting at a vertex with a source or sink at the vertex, Jeffery–Hamel flows are the exact similarity solution as the NSE [2]. The interplay between the magnetic characteristics and the behaviour of electrically conducting fluids is described by magnetohydrodynamics (MHD). Electrically conducting non-Newtonian fluid flow is important because in most practical circumstances, fluids behave differently under the influence of magnetic fields than nonconductive fluid [3]. The magnetohydrodynamic (MHD) direction of the flow should also be considered in these cases [3]. The most recent works on magnetic blood flow are given in [4–6].

Some numerical methods for situations involving Jeffery–Hamel flows have been developed in the literature. Khan et al. [3] investigated the equations that regulate the slip effects on Casson fluid MHD flow in converging/diverging channels. First, they used a suitable similarity transformation to convert the system of governing nonlinear partial differential equations to a system of ordinary differential equations. The final problem was then solved using Adomian's decomposition method and the variation of parameters method. They discovered that raising parameter values causes the velocity in the narrowing channel and the velocity in the widening channel to behave in opposing ways. They found, on the other hand, that the Casson fluid's hydrodynamic slip flow can be exploited to stop the separation phenomenon in the diverging channel. Hamrelaine et al. [7] investigated the third-order MHD Jeffery–Hamel flow with suction/injection. The homotopy analysis method (HAM) was used to obtain a semianalytic solution, and the Runge–Kutta method is used to calculate a numerical solution. A comparison of the methodologies was carried out. They discovered that the analytical and numerical outcomes are similar. Ara et al. [8] studied the Jeffery–Hamel flow of an incompressible non-Newtonian fluid inside nonparallel walls. They converted the governing nonlinear partial differential equations to nonlinear coupled ordinary differential equations and implemented the Taylor optimization method to get the analytic solution. The results agree with those of the Runge–Kutta method. Heat transfer in a two-dimensional magnetohydrodynamic viscous incompressible flow in convergent/divergent channels was studied by Mahmood et al. [9]. They used the spectral homotopy analysis method (SHAM) to solve the governing nonlinear differential equations and found that increasing the Reynold number, Prandtl number, or Nusselt number yields an increase in the temperature profile. Recently, Adel et al. [10] implemented a Bernoulli collocation method to provide a numerical simulation of the Jeffery–Hamel blood flow problem.

The goal of this research is to use a numerical technique based on the Bernstein collocation method to investigate a solution for the MHD Jeffery–Hamel blood flow problem. The polynomials determined in the Bernstein basis are widely used in a variety of applications because Bernstein polynomials are used as base polynomials since they are dense in L^2 and hence produce good approximation results [11]. The Bernstein polynomial $B_n f(x)$ converges uniformly to $f(x)$ on [0, 1] by the Weierstrass theorem [12]. We shall note that if the solution of the differential equation is a polynomial of degree n, then the Bernstein collocation method will give the exact solution [12]. Jafarian et al. [13] presented approximate solutions of the Fredholm and Volterra integral equation systems of the second kind by an application of the Bernstein polynomials expansion method. In this technique, the original integral equation system is reduced to a linear system from which the unknown Bernstein coefficients of the solutions can be easily obtained. Recently, the regularized and the modified regularized long wave (RLW and MRLW) equations have been solved by Hammad [14] using the Bernstein collocation method. He managed to reduce the equations to a system of nonlinear algebraic equations which is easier to solve than the original equations. In addition, the general form of any derivative of Bernstein polynomials was also given for the first time in [14]. The Bernstein collocation method has also been applied to solve functional differential equations of neutral type with good outcomes [15], to find an approximate solution of the fractional equal width wave equation and the modified equal width wave equation [16], and in many interesting problems in science, engineering, and medical fields [17–20]. By using the Bernstein collocation method, the problem is transformed into a nonlinear system of algebraic equations. The residual correction procedure is used to estimate the error; it is simple to use and can be used even when the exact solution is unknown. In addition, the corrected Bernstein solution can be found. Moreover, the accuracy and efficiency of the proposed method are evaluated by applying the one-way ANOVA analysis which has been applied by Ahmad and Ilyas [21].

The following is a breakdown of the paper's structure. The governing equation and problem statement are given in Section 2. The definitions and formulations of Bernstein polynomials are given in Section 3. Then, the BCM is introduced by defining the residual function. In Section 4, an error estimation procedure and a residual correction procedure are given. Some examples to illustrate how the method works are shown in Section 5. A comparison of the BCM against the HPM [21] will also be presented. The last section summarizes the results.

2. Governing Equation and Problem Formulation

The nonlinear MHD Jeffery–Hamel arterial blood flow problem was given in [1, 2, 21]. Consider a continuous two-dimensional flow of an incompressible conducting viscous fluid from a source or sink at channel walls lying in planes with an angle of 2α, as illustrated in Figure 1. Using the continuity Navier–Stokes equations in polar coordinates and assuming that the velocity is exclusively along the radial direction and relies on r and θ, the governing equations are as follows [22]:

$$\frac{\rho}{r}\frac{\partial}{\partial r}\left(r\cdot u(r,\theta)\right)=0, \tag{1}$$

$$u(r,\theta)\frac{\partial u(r,\theta)}{\partial r}=-\frac{1}{\rho}\frac{\partial P}{\partial r}+\nu\left[\frac{\partial^2 u(r,\theta)}{\partial r^2}+\frac{1}{r}\frac{\partial u(r,\theta)}{\partial r}+\frac{1}{r^2}\frac{\partial^2 u(r,\theta)}{\partial\theta^2}-\frac{u(r,\theta)}{r^2}\right], \tag{2}$$

$$\frac{1}{\rho r}\frac{\partial P}{\partial\theta}-\frac{2\nu\rho}{r}\frac{\partial u(r,\theta)}{\partial\theta}=0, \tag{3}$$

subject to the boundary conditions,

$$\begin{aligned}\frac{\partial u(r,\theta)}{\partial\theta}&=0,\quad \text{at the centerline of the channel,}\\ u(r,\theta)&=0,\quad \text{at the walls of the channel.}\end{aligned} \tag{4}$$

The fluid density, pressure of the fluid, and coefficient of kinematics viscosity are represented by ρ, P, ν, respectively. In a cylindrical coordinate, the artery was assumed to have a constant cross-sectional area and no viscoelastic impact.

2.1. Problem Formulation. Following Ahmad and Ilyas [21], problems (1)–(3) can be reduced to a nonlinear ordinary differential equation. First, integrating the equation of continuity with respect to r,

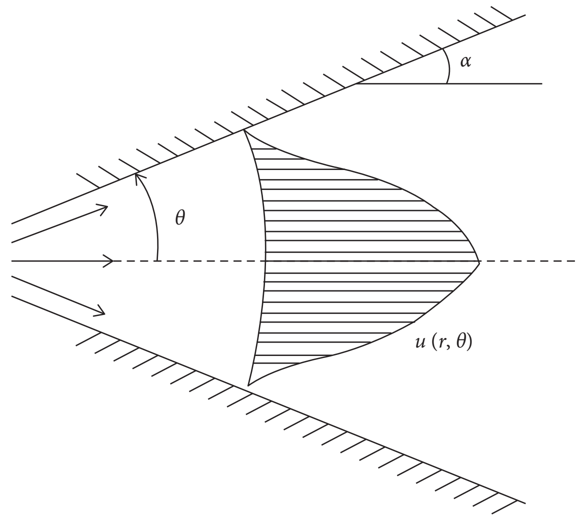

Figure 1: The physical geometry of the Jeffery–Hamel flow problem.

$$\left(\frac{\rho}{r}\right)\frac{\partial}{\partial r}\left[r\left[u\left(r,\theta\right)\right]\right]=0. \quad (5)$$

Yields as

$$ru\left(r,\theta\right)=\varphi\left(\theta\right). \quad (6)$$

Let

$$\varphi\left(\eta\right)=\frac{\varphi\left(\theta\right)}{A}, \quad (7)$$

where

$$\eta=\frac{\theta}{\alpha}, \qquad A=\varphi_{\max}. \quad (8)$$

Then, let us obtain the following functions written in terms of φ:

$$\frac{\partial u\left(r,\theta\right)}{\partial r}=-\frac{A\varphi\left(\eta\right)}{r^{2}}, \quad (9)$$

$$\frac{\partial^{2}u\left(r,\theta\right)}{\partial r^{2}}=\frac{2A\varphi\left(\eta\right)}{r^{3}}, \quad (10)$$

$$\frac{\partial u\left(r,\theta\right)}{\partial\theta}=\frac{A\varphi\prime\left(\eta\right)}{r\alpha}, \quad (11)$$

$$\frac{\partial^{2}\left(r,\theta\right)}{\partial\theta^{2}}=\frac{A\varphi\prime\prime\left(\eta\right)}{r\alpha^{2}}. \quad (12)$$

Integrating and simplifying (3) with respect to θ gives pressure as follows:

$$P=\frac{2\nu}{r}\rho u\left(r,\theta\right). \quad (13)$$

We obtain the following equation by differentiating P with respect to r and by using (8):

$$\frac{1}{\rho}\frac{\partial P}{\partial r}=-\frac{4\nu A\varphi\left(\eta\right)}{r^{3}}. \quad (14)$$

Substituting (9)–(14) into (3), we get

$$-\frac{A^{2}\varphi^{2}\left(\eta\right)}{r^{3}}=\frac{4\nu A\varphi\left(\eta\right)}{r^{3}}+\nu\left[\frac{2A\varphi\left(\eta\right)}{r^{3}}-\frac{1}{r}\frac{A\varphi\left(\eta\right)}{r^{2}}+\frac{1}{r^{3}}\frac{A\varphi\prime\prime\left(\eta\right)}{\alpha^{2}}-\frac{A\varphi\left(\eta\right)}{r^{3}}\right], \quad (15)$$

or simply

$$A\varphi^{2}\left(\eta\right)+4\nu A\varphi\left(\eta\right)+\nu\frac{A\varphi\prime\prime\left(\eta\right)}{\alpha^{2}}=0. \quad (16)$$

Differentiating (16) with respect to η, we get

$$\varphi'''\left(\eta\right)+2\alpha\operatorname{Re}\varphi\left(\eta\right)\varphi'+4\alpha^{2}\varphi'\left(\eta\right)=0. \quad (17)$$

Subject to the boundary conditions,

$$\varphi\left(0\right)=1, \qquad \varphi\prime\left(0\right)=0, \qquad \varphi\left(1\right)=0, \quad (18)$$

where prime denotes derivative with respect to η, and α is the angle between the inclined plates. Here,Re is the Reynolds number which is defined as follows [2]:

$$Re=\frac{\alpha\varphi_{\max}}{\nu}=\frac{r\alpha U_{\max}}{\nu}\begin{pmatrix}\text{divergent channel: } \alpha>0, U_{\max}>0\\ \text{convergent channel: } \alpha<0, U_{\max}<0\end{pmatrix}, \quad (19)$$

and $U_{\max}$ is the maximum velocity at the centre of the channel ($r=0$). Note that the solution $\varphi\left(\eta\right)$ of equation (17) is related to the solution $u\left(r,\theta\right)$ of the original PDEs via the following relation obtained from equations (6) and (7) as follows:

$$\varphi(\eta) = \frac{\varphi(\theta)}{A} = \frac{ru(r,\theta)}{A}. \tag{20}$$

From which $u(r,\theta) = (A/r)\varphi(\eta)$. We can use the form of solution as given in equation (20) since in the Jeffery–Hamel flow, the velocity is exclusively along the radial direction.

3. Bernstein Collocation Method (BCM)

In this section, Bernstein polynomials on the interval $[0,1]$ are defined and the basic ideas of the approximating functions using BCM are introduced.

Definition 1. The Bernstein polynomials of degree m defined on the interval $[0,1]$ are given as [23, 24]

$$B_{i,m}(\eta) = \binom{m}{i}(\eta)^i(1-\eta)^{m-i}, \quad i = 0,1,\ldots,m, \tag{21}$$

where the binomial coefficient is

$$\binom{m}{i} = \frac{m!}{i!(m-i)!}. \tag{22}$$

For convenience, set $B_{i,m} = 0$ if $i < 0$ or $i > m$.

Let $\varphi(\eta)$ be the exact solution of (17) and (18). Approximate $\varphi(\eta)$ by BCM as follows:

$$\varphi(\eta) \simeq \varphi_m(\eta) = \sum_{i=0}^{m} c_i B_{i,m}(\eta) = C\Phi(\eta), \tag{23}$$

where C is an unknown constant matrix of size $1\times(m+1)$ to be determined and $\Phi(\eta)$ is a matrix of size $(m+1)\times 1$, consisting of the Bernstein basis polynomial elements, defined, respectively, as follows:

$$C = [c_0,\ldots,c_m]_{1\times(m+1)}, \quad \Phi(\eta) = [B_{0,m}(\eta), B_{1,m}(\eta),\ldots,B_{m,m}(\eta)]_{(m+1)\times 1}. \tag{24}$$

The n-th derivatives of $\varphi(\eta)$ can be expressed directly from the Bernstein basis polynomial elements as

$$\varphi\prime(\eta) \simeq \varphi_m'(\eta) = C\Phi\prime(\eta),\ldots,\varphi^{(n)}(\eta) \simeq \varphi_m^{(n)}(\eta) = C\Phi^{(n)}(\eta). \tag{25}$$

To solve equation (17) subject to the boundary conditions (15) by means of BCM, first substitute equations (23)–(25) into equation (17) to get the residual function $\mathrm{Re}(\eta)$,

$$\mathrm{Re}(\eta) = C\Phi\prime\prime\prime(\eta) + 2\alpha\mathrm{Re}\, C\Phi(\eta)C\Phi\prime(\eta) + 4\alpha^2 C\Phi\prime(\eta). \tag{26}$$

Now, replacing η by η_i and then applying the collocation nodes

$$\eta_i = \frac{1}{2} + \frac{1}{2}\cos\left(\frac{(2i+1)\pi}{2(m-1)}\right), \quad i = 0,1,\ldots,m-2. \tag{27}$$

On equation (26) generates $(m-1)$ set of linear or nonlinear algebraic equations. On the other hand, by imposing again equations (23)–(25) to the boundary conditions (18) as

$$\varphi_m(0) = C\Phi(0) = 1, \quad \varphi_m'(0) = C\Phi\prime(0) = 0, \quad \varphi_m(1) = C\Phi(1) = 0, \tag{28}$$

Finally, generate $(m+1)$ set of linear or nonlinear algebraic equations. The solution of this set of linear or nonlinear algebraic equations gives the unknown coefficients of the vector C. Consequently, $\varphi_m(\eta)$ given in equation (23) is obtained once C is known.

4. Error Estimates and Residual Correction Procedure

In this section, the procedure presented in the work of Bataineh et al. [25] will be adopted and the error estimations for BCM solutions using the residual correction procedure shall be given.

Let $\varphi(\eta)$ and $\varphi_m(\eta)$ be the exact solution and the BCM solutions of equation (17), respectively, then define the error function $e(\eta)$ as $e(\eta) = \varphi(\eta) - \varphi_m(\eta)$. Now, let us constitute the residual correction procedure for the method. First, substituting the term $\varphi(\eta) = e(\eta) + \varphi_m(\eta)$ into equation (17) yields

$$(e(\eta) + \varphi_m(\eta))\prime\prime\prime + 2\alpha\mathrm{Re}(e(\eta) + \varphi_m(\eta)) \cdot (e(\eta) + \varphi_m(\eta))\prime\prime + 4\alpha^2(e(\eta) + \varphi_m(\eta))\prime = 0. \tag{29}$$

By applying the method for a given value of n to equation (29) subject to the boundary conditions

$$e_n(0) = \widehat{C}\Phi(0) - \varphi_m(0), e_n'(0) = \widehat{C}\Phi\prime(0) - \varphi_m'(0), e_n(1) = \widehat{C}\Phi(1) - \varphi_m(1). \tag{30}$$

The approximate solution $e_n(\eta) = \widehat{C}\Phi(\eta)$ for the error will be obtained. Note that the polynomial $\varphi_m(\eta) + e_n(\eta)$ is an approximate solution of (17). Here, $\varphi_m^n(\eta) = \varphi_m(\eta) + e_n(\eta)$ is the corrected BCM solution.

Corollary 1. *If $\varphi_m(\eta)$ is the approximate solution of (17), then $\varphi_m^n(\eta)$ is also an approximate solution of (17). Moreover, $\varphi_m^n(\eta)$ is a better approximation than $\varphi_m(\eta)$ provided that*

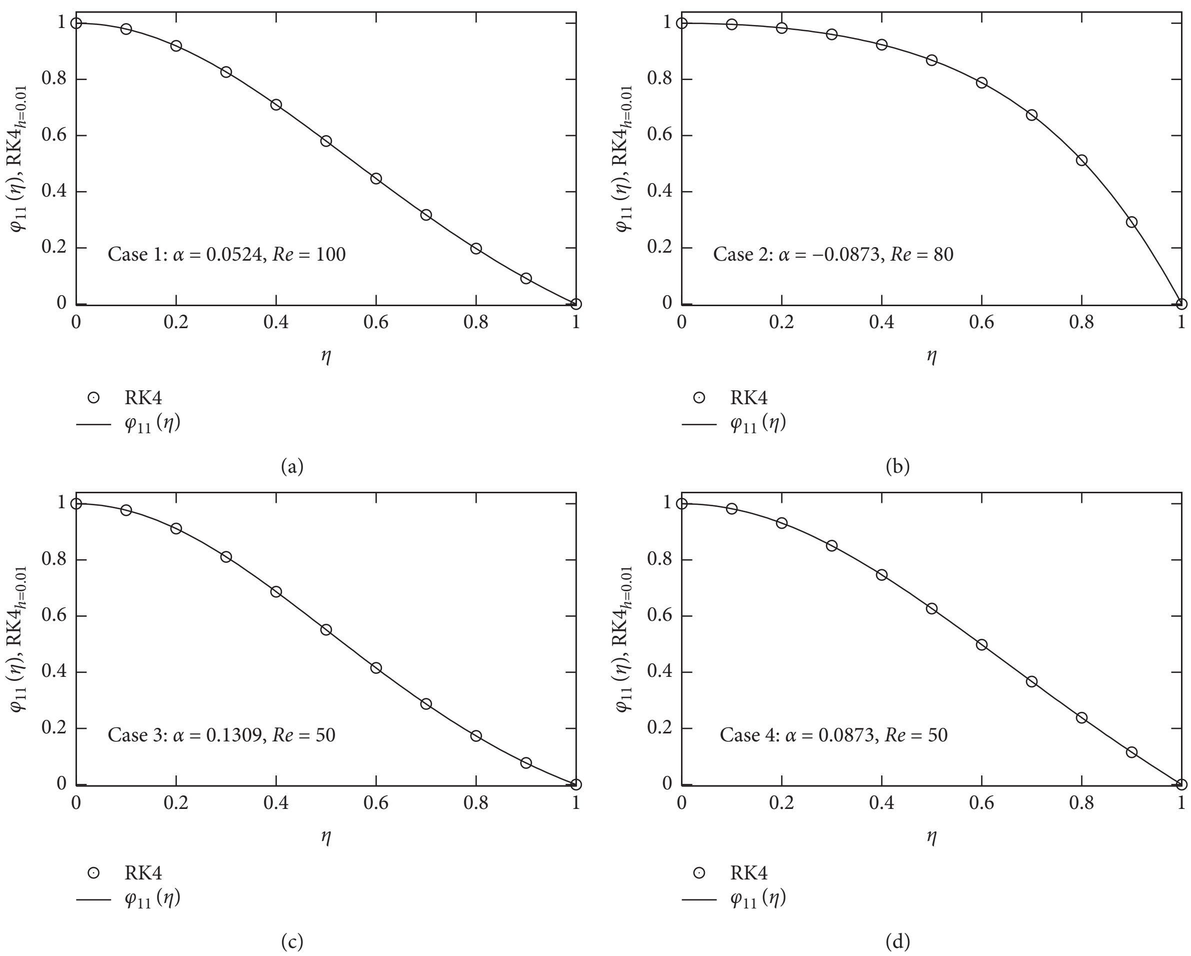

Figure 2: Numerical results of BCM plotted against the RK4 for the four cases.

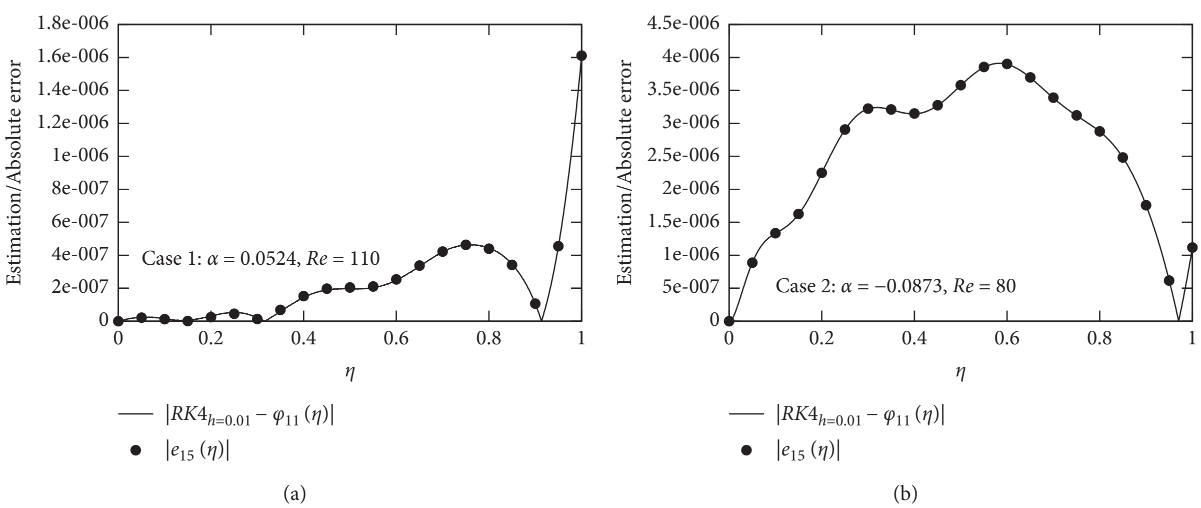

Figure 3: Continued.

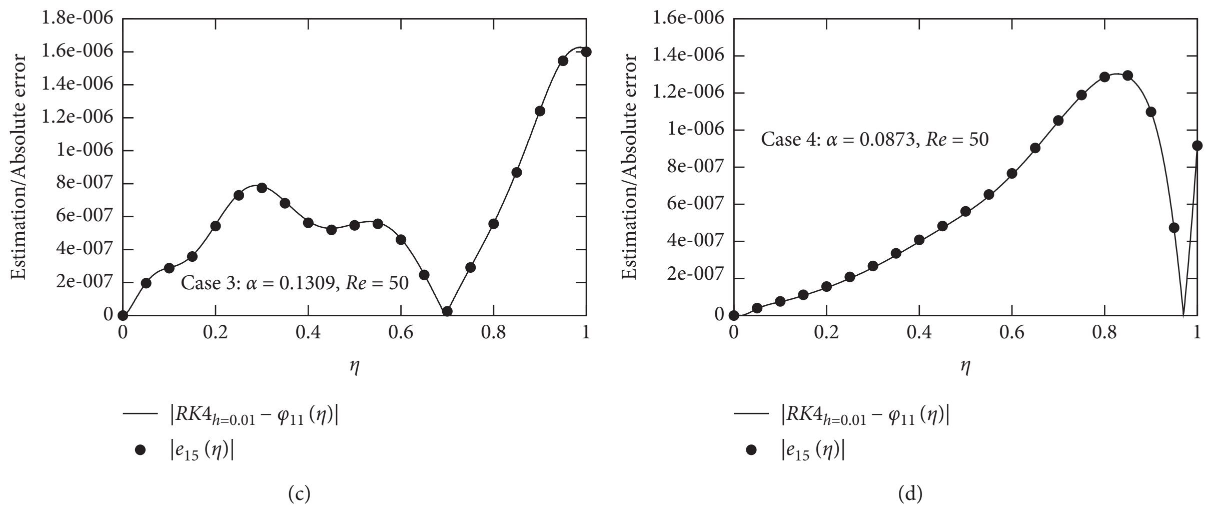

Figure 3: Numerical results of BCM for different cases.

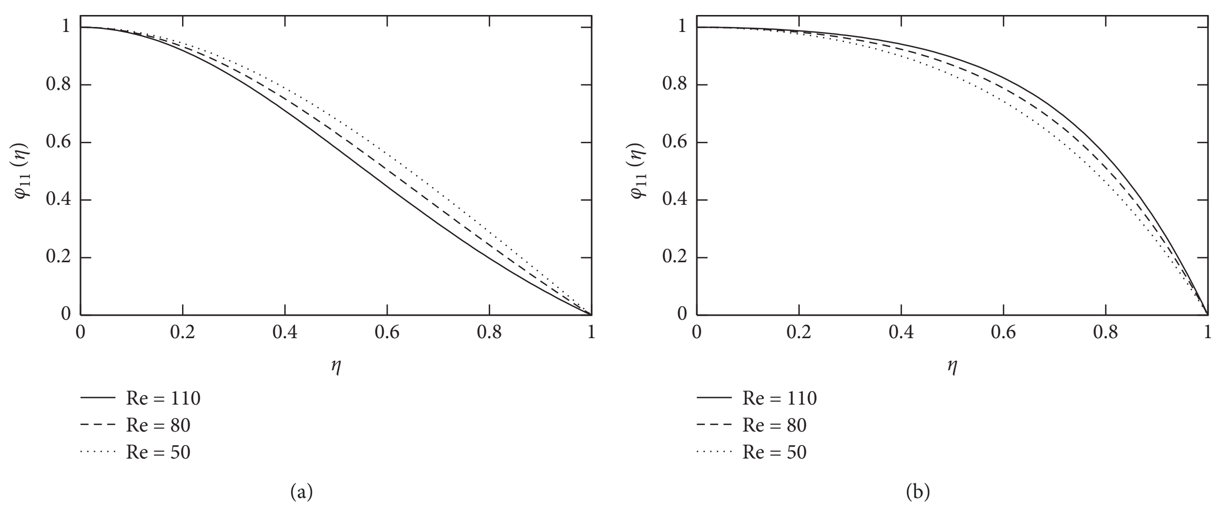

Figure 4: Velocity diagram via BCM for different values of Re when (a) $\alpha = 0.0524$and (b) $\alpha = -0.0873$.

$$\begin{aligned}\left\|\varphi(\eta)-\varphi_m^n(\eta)\right\| &= \left\|\varphi(\eta)-\varphi_m(\eta)-e_n(\eta)\right\| \\ &= \left\|e(\eta)-e_n(\eta)\right\| < \left\|\varphi(\eta)-\varphi_m(\eta)\right\|.\end{aligned} \tag{31}$$

5. Numerical Experiments

In this section, the present method is applied to the Jeffery–Hamel blood flow problem for four different cases: Case 1 $(\alpha = 0.0524, \mathrm{Re} = 110)$, Case 2 $(\alpha = -0.0873, \mathrm{Re} = 80)$, Case 3 $(\alpha = 0.1309, \mathrm{Re} = 50)$, and Case 4 $(\alpha = 0.0873, \mathrm{Re} = 50)$ [21]. Since the exact solutions are unknown, the approximate solutions obtained by the fourth-order Runge–Kutta (RK4) method is taken as the reference solutions.

The solutions obtained by BCM and RK4 with step size $h = 0.01$ are given in Figure 2. The absolute errors and their estimations obtained by the residual correction procedure are shown in Figure 3. As shown in Figure 2, increasing η yields a decrease in the flow rate of blood for four cases. Moreover, any changes in Re and α lead to a change in the flow rate of blood. For all the cases considered, the results obtained by the BCM match very well with the results obtained by RK4. Observe from Figure 3 that the estimations of absolute errors agree well with the absolute errors. Figures 4 and 5 show the impact of the Reynolds number and the steep angle of the channel on the fluid velocity profile. It can be concluded that, when $\alpha < 0$ and the channel's steepness is divergent, an increase in Reynolds number causes a decrease in velocity as shown in Figure 4(a), the findings are inverse when $\alpha > 0$ and the steepness of the channel is convergent. An increase in Reynolds number leads to an increase in velocity as shown in Figure 4(b) and as shown in Figures 5(a) and 5(b), the divergence angle of the channel and the velocity of the fluid have an inverse relationship when the Reynolds number is fixed.

The BCM solutions for the four cases are listed in Table 1. The absolute errors with a comparison with the HPM [21] are given in Table 2. As shown in Table 2, the approximations obtained by the BCM are more accurate than the

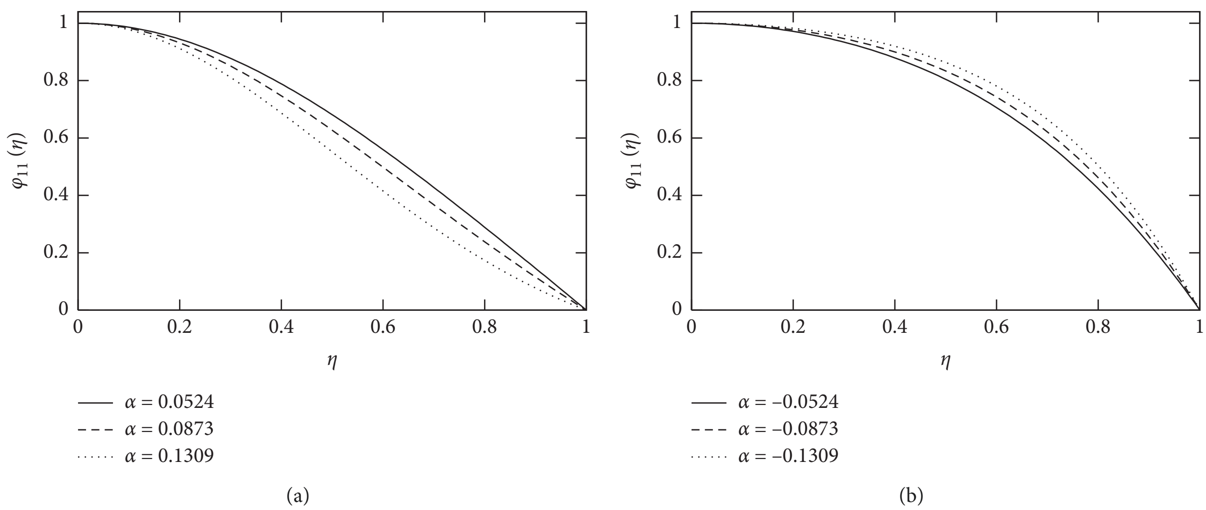

Figure 5: Velocity diagram via BCM for different values of α when Re = 50.

Table 1: A comparison of approximate solutions of the BCM $\varphi_{11}(\eta)$ with corrected approximate solutions $\varphi_{11}(\eta) + e15(\eta)$ for the four cases.

η	BCM	Corrected BCM	BCM	Corrected BCM
	Case 1		Case 2	
0.0	1.000000000	1.0000000000	1.000000000	1.0000000000
0.2	0.919225399	0.9192254258	0.983283205	0.9832809532
0.4	0.710099389	0.7100992462	0.923545641	0.9235424804
0.6	0.446767409	0.4467672312	0.788136035	0.7881322939
0.8	0.197511261	0.197511191	0.512041076	0.5120402409
1.0	-1.34×10^{-5}	0.0000000000	-6.41×10^{-5}	0.0000000000
	Case 3		Case 4	
0.0	1.0000000000	1.0000000000	1.0000000000	1.0000000000
0.2	0.911478534	0.9114790754	0.9312123216	0.9312121687
0.4	0.686913821	0.6869143720	0.7467483082	0.7467479488
0.6	0.415107740	0.4151082910	0.4981734784	0.4981730282
0.8	0.173121071	0.1731216776	0.2380746233	0.2380742195
1.0	-4.92×10^{-5}	0.0000000000	-6.02×10^{-5}	0.0000000000

Table 2: Absolute errors of BCM and HPM [21].

η	BCM	HPM [21]	BCM	HPM [21]
	Case 1		Case 2	
0.0	0	0	0	0
0.2	3.23×10^{-8}	7.92×10^{-3}	2.25×10^{-6}	2.24×10^{-4}
0.4	1.36×10^{-7}	2.87×10^{-2}	3.16×10^{-6}	9.90×10^{-4}
0.6	2.00×10^{-7}	5.68×10^{-2}	3.85×10^{-6}	2.11×10^{-3}
0.8	2.83×10^{-7}	7.57×10^{-2}	2.01×10^{-6}	1.30×10^{-3}
1.0	1.34×10^{-6}	9.17×10^{-9}	6.41×10^{-6}	6.30×10^{-8}
	Case 3		Case 4	
0.0	0	0	0	0
0.2	5.50×10^{-7}	1.42×10^{-2}	1.47×10^{-7}	2.30×10^{-3}
0.4	5.67×10^{-7}	5.11×10^{-2}	3.51×10^{-7}	8.53×10^{-3}
0.6	6.05×10^{-7}	9.94×10^{-2}	4.28×10^{-7}	1.74×10^{-2}
0.8	7.51×10^{-7}	1.29×10^{-1}	1.11×10^{-7}	2.42×10^{-2}
1.0	4.92×10^{-6}	7.88×10^{-9}	2.90×10^{-6}	1.03×10^{-8}

Table 3: A comparison of absolute error of corrected BCM solutions $|\varphi_{11}(\eta) + e_{15}(\eta) - \text{RK4}|$ with absolute error of HPM solutions [21] for the cases.

η	Corrected BCM	HPM [21]	Corrected BCM	HPM [21]
	Case 1		Case 2	
0.0	0	0	0	0
0.2	6.27×10^{-9}	7.91×10^{-3}	4.32×10^{-9}	2.24×10^{-4}
0.4	7.29×10^{-9}	2.87×10^{-2}	4.76×10^{-9}	9.90×10^{-4}
0.6	2.22×10^{-8}	5.68×10^{-2}	5.42×10^{-9}	2.11×10^{-3}
0.8	2.14×10^{-7}	7.57×10^{-2}	3.63×10^{-9}	1.30×10^{-3}
1.0	1.00×10^{-6}	9.17×10^{-9}	7.27×10^{-9}	6.30×10^{-8}
	Case 3		Case 4	
0.0	0	0	0	0
0.2	8.02×10^{-9}	1.42×10^{-2}	6.13×10^{-9}	2.30×10^{-3}
0.4	1.05×10^{-8}	5.11×10^{-2}	1.01×10^{-8}	8.53×10^{-3}
0.6	6.26×10^{-9}	9.94×10^{-2}	8.45×10^{-9}	1.74×10^{-2}
0.8	2.18×10^{-9}	1.29×10^{-1}	1.11×10^{-9}	2.42×10^{-2}
1.0	1.17×10^{-9}	7.88×10^{-9}	5.29×10^{-10}	1.03×10^{-8}

Table 4: Results of ANOVA for BCM.

Source	df	Adj SS	Adj MS	F-value	p value
Factor	3	0.000	0.000	7.060	0.001
Error	40	0.000	0.000		
Total	43	0.000	0.000		

approximations obtained by the HPM for all the cases studied. The corrected BCM solutions with a comparison by HPM [21] are also given in Table 1. As shown in Table 3, the corrected BCM solutions are much more accurate than both the BCM and the HPM [21] solutions for all the cases.

One-way ANOVA analysis was conducted to determine whether there was any statistically significant difference between the absolute errors or not. A Tukey analysis from post hoc tests was also conducted to determine group

Table 5: Tukey results for BMP.

		Mean			95% confidence int.	
Case	Cases	Difference	Std. error	Sig.	Lower bound	Upper bound
1	2	−0.00002270*	0.000005311	0.001	−0.00003694	−0.00000846
	3	−0.00000693*	0.000005311	0.565	−0.00002117	0.000007302
	4	−0.00000376*	0.000005311	0.893	−0.00001800	0.000010479
2	3	0.00001577*	0.000005311	0.025	0.000001529	0.000030003
	4	0.00001894*	0.000005311	0.005	0.000004706	0.000033179
3	4	0.000003177*	0.000005311	0.932	−0.00001106	0.000017414

**The mean difference is significant at the 0.05 level

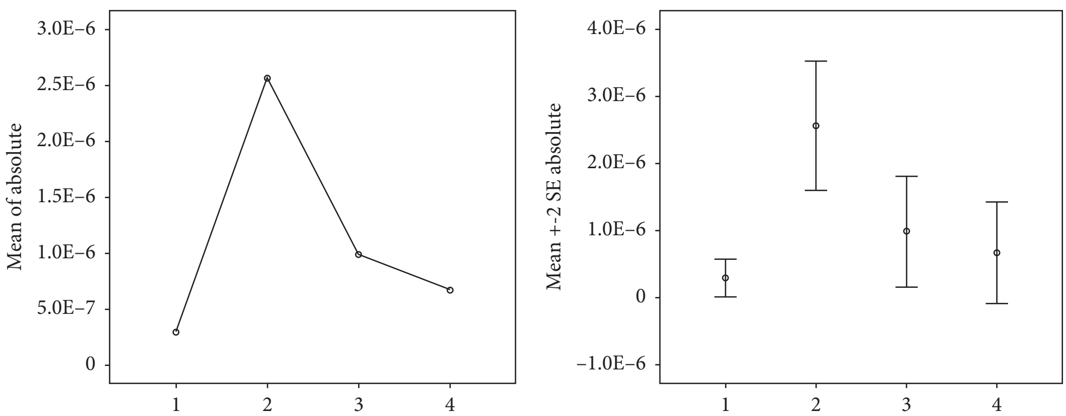

(a) (b)

Figure 6: (a) The mean of the absolute errors for BCM. (b) The mean ±2SE of the absolute errors for BCM.

differences. The SPSS 22 program for the statistical analysis was used. Analysis results are given in Tables 4 and 5. According to the ANOVA results in Table 4, there is a significant difference between at least two groups ($F_{(3-40)} = 7.060$, $p < 0.05$). The Tukey pairwise comparison results show that Case 2 is different from the other groups. Contrary to the HPM [21] results, it is seen from Figure 6 that the mean of the absolute errors for Case 2 is different from the means of the other groups.

6. Conclusions

In this study, the Bernstein collocation method (BCM) has been applied to solve the MHD Jeffery–Hamel blood flow problem. The original two-dimensional blood flow problem was first reduced to a one-dimensional third-order nonlinear differential equation (ODE) by applying some transformation rules. Using the BCM, the nonlinear ODE was then converted to a system of nonlinear algebraic equations. The Bernstein approximate solutions were improved by the residual correction procedure. This procedure was applied to estimate the error and to get more accurate approximations, namely, corrected BCM solutions. The method was tested on the problem for some different values of Re and α. After applying the method to the examples, it was found that the present method is better than HPM [21]. On the other hand, the residual correction procedure estimates the error well. As a result, more accurate approximations can be obtained by using the procedure. As a result of the statistical analysis, Case 2 is different from the other groups for the BCM.

Abbreviations

ρ: Fluid density
r, θ: Cylindrical coordinates
P: Pressure term
ν: Kinematic viscosity
α: Angle of the channel
$U_{\max}$: Maximum value of velocity
η and A: Dimensionless parameters
Re: Reynolds number.

Data Availability

The study did not report any data.

Consent

Consent is not applicable in this study.

Conflicts of Interest

The authors declare no conflicts of interest.

Authors' Contributions

A.S.B. contributed to the conceptualization of the study; A.S.B. and O.R.I. contributed to the methodology; A.S.B.

and O.R.I. were responsible for software; A.S.B., O.R.I., and I.H. contributed to the validation; A.S.B. and O.R.I. were responsible for formal analysis; A.S.B. contributed to the original draft preparation; A.S.B., O.R.I., and I.H. contributed to reviewing and editing; and I.H. was responsible for funding acquisition. All authors have read and agreed to the published version of the manuscript.

Acknowledgments

Prof. Dr. Ahmad Sami Bataineh would like to thank Al-Balqa Applied University for providing him with a sabbatical leave at Universiti Kebangsaan Malaysia which allowed him to conduct this research. The APC was funded by Universiti Kebangsaan Malaysia (Grant # DIP-2021-018).

References

[1] G. B. Jeffery, "L The two-dimensional steady motion of a viscous fluid," *The London, Edinburgh, and Dublin Philosophical Magazine and Journal of Science*, vol. 29, no. 172, pp. 455–465, 1915.

[2] V. Marinca and N. Herişanu, "An optimal homotopy asymptotic approach applied to nonlinear MHD Jeffery-Hamel flow," *Mathematical Problems in Engineering*, vol. 2011, Article ID 169056, 16 pages, 2011.

[3] U. Khan, W. Sikandar, N. Ahmed, S. T. M. Din, and N. Ahmed, "Effects of velocity slip on MHD flow of a non-Newtonian fluid in converging and diverging channels," *International Journal of Algorithms, Computing and Mathematics*, vol. 2, no. 4, pp. 469–483, 2016.

[4] D. F. Jamil, S. Saleem, R. Roslan et al., "Analysis of non-Newtonian magnetic Casson blood flow in an inclined stenosed artery using Caputo-Fabrizio fractional derivatives," *Computer Methods and Programs in Biomedicine*, vol. 203, Article ID 106044, 2021.

[5] M. Nazeer, S. Saleem, F. Hussain, S. Iftikhar, and A. A. Qahtani, "Mathematical modeling of bio-magnetic fluid bounded by ciliated walls of wavy channel incorporated with viscous dissipation: discarding mucus from lungs and blood streams," *International Communications in Heat and Mass Transfer*, vol. 124, Article ID 105274, 2021.

[6] M. Qasim, M. I. Afridi, A. Wakif, and S. Saleem, "Influence of variable transport properties on nonlinear radioactive Jeffrey fluid flow over a disk: utilization of generalized differential quadrature method," *Arabian Journal for Science and Engineering*, vol. 44, no. 6, 2019.

[7] S. Hamrelaine, F. M. Oudina, and M. Rafik, "Analysis of MHD Jeffery-Hamel flow with suction/injection by homotopy analysis method," *J. Adv. Res. Fluid Mech. Therm. Sci.*vol. 58, pp. 173–186, 2019.

[8] A. Ara, N. A. Khan, F. Naz, M. A. Z. Raja, and Q. Rubbab, "Numerical simulation for Jeffery-Hamel flow and heat transfer of micropolar fluid based on differential evolution algorithm," *AIP Advances*, vol. 8, no. 1, Article ID 015201, 2018.

[9] A. Mahmood, M. F. M. Basir, U. Ali, M. S. M. Kasihmuddin, and M. A. Mansor, "Numerical solutions of heat transfer for magnetohydrodynamic Jeffery-Hamel flow using spectral homotopy analysis method," *Processes*, vol. 7, no. 9, 626 pages, 2019.

[10] W. Adel, K. E. Biçer, and M. Sezer, "A novel numerical approach for simulating the nonlinear MHD Jeffery-Hamel flow problem," *International Journal of Algorithms, Computing and Mathematics*, vol. 7, no. 3, pp. 74–15, 2021.

[11] L. Coluccio, A. Eisinberg, and G. Fedele, "Gauss-Lobatto to Bernstein polynomials transformation," *Journal of Computational and Applied Mathematics*, vol. 222, no. 2, pp. 690–700, 2008.

[12] G. G. Lorentz, *Bernstein Polynomials*, American Mathematical Soc, Providence, RI, USA, 2013.

[13] A. Jafarian, S. A. M. Nia, A. K. Golmankhaneh, and D. Baleanu, "Numerical solution of linear integral equations system using the Bernstein collocation method," *Advances in Difference Equations*, vol. 2013, no. 1, 123 pages, 2013.

[14] D. A. Hammad, "Application of Bernstein collocation method for solving the generalized regularized long wave equations," *Ain Shams Engineering Journal*, vol. 12, no. 4, pp. 4081–4089, 2021.

[15] I. Ali, "Bernstein collocation method for neutral type functional differential equation," *Mathematical Biosciences and Engineering*, vol. 18, no. 3, pp. 2764–2774, 2021.

[16] S. H. Mohammad and E. S. A. Rawi, "Solving fractional coupled EW and coupled MEW equations using Bernstein collocation method," *Journal of Physics: Conference Series*, vol. 1804, Article ID 012021, 2021.

[17] A. S. Bataineh, O. R. Isik, M. A. N. Oqielat, and I. Hashim, "An enhanced adaptive Bernstein collocation method for solving systems of ODEs," *Mathematics*, vol. 9, no. 4, p. 425, 2021.

[18] J. Shahni and R. Singh, "Numerical solution of system of Emden-Fowler type equations by Bernstein collocation method," *Journal of Mathematical Chemistry*, vol. 59, no. 4, pp. 1117–1138, 2021.

[19] J. Shahni and R. Singh, "An efficient numerical technique for Lane-Emden-Fowler boundary value problems: Bernstein collocation method," *The European Physical Journal Plus*, vol. 135, no. 6, 475 pages, 2020.

[20] J. Shahni and R. Singh, "Numerical results of Emden-Fowler boundary value problems with derivative dependence using the Bernstein collocation method," *Engineering with Computers*, vol. 38, pp. 371–380, 2022.

[21] I. Ahmad and H. Ilyas, "Homotopy perturbation method for the nonlinear MHD Jeffery-Hamel blood flows problem," *Applied Numerical Mathematics*, vol. 141, pp. 124–132, 2019.

[22] H. Schlichting and K. Gersten, *Boundary-layer Theory*, McGraw-Hill, New York, NY, USA, 2000.

[23] M. I. Bhatti and P. Bracken, "Solutions of differential equations in a Bernstein polynomial basis," *Journal of Computational and Applied Mathematics*, vol. 205, no. 1, pp. 272–280, 2007.

[24] A. Dascioglu and N. Isler, "Bernstein collocation method for solving nonlinear differential equations," *Mathematical and Computational Applications*, vol. 18, no. 3, pp. 293–300, 2013.

[25] A. S. Bataineh, O. R. Isik, and I. Hashim, "Bernstein method for the MHD flow and heat transfer of a second grade fluid in a channel with porous wall," *Alexandria Engineering Journal*, vol. 55, no. 3, pp. 2149–2156, 2016.